

Dielectric breakdown in MgO-barrier magnetic tunnel junctions with a CoFeB based synthetic ferrimagnetic recording layer

M. Yamanouchi¹, Y. Mori², J. Hayakawa¹, H. Yamamoto¹, K. Miura¹, H. Hasegawa³, K. Ito¹, K. Takeda², K. Meguro², H. Takahashi¹, H. Matsuoka¹, S. Ikeda³, and H. Ohno³

¹Advanced Research Laboratory, Hitachi, Ltd., Kokubunji, Tokyo 185-8601, Japan

Phone: +81-42-323-1111 E-mail: michihiko.yamanouchi.cg@hitachi.com

²Central Research Laboratory, Hitachi, Ltd., Kokubunji, Tokyo 185-8601, Japan

³Laboratory for Nanoelectrics and Spintronics Research Institute of Electrical Communication, Tohoku University, 2-1-1 Katahira, Aobaku, Sendai 980-8577, Japan

1. Introduction

Spin-transfer torque RAM (SPRAM) [1] is attracting much interest as a candidate for universal memory because of its potential for providing a non-volatile, high speed, and low power consumption RAM. A memory cell of the SPRAM consists of a magnetic tunnel junction (MTJ) and a selecting transistor. For the SPRAM, MgO-barrier MTJs with a synthetic ferrimagnetic (SyF) recording layer are promising because the SyF allows us to reduce writing current while maintaining high thermal stability [2]. The reliability of the barrier, however, has not been understood. Moreover, because a current pulse with the amplitude of a few MA/cm² is applied to the MTJ in a writing operation, understanding the dielectric breakdown in the MTJs is essential. To characterize the dielectric breakdown, distributions of time-to-breakdown (t_{BD}) under accelerated stress conditions are measured. From the dependence of the distributions on the stress conditions, the lifetime of the MTJ under an operating condition is extrapolated [3]. In this work, we have investigated distributions of t_{BD} in MgO-barrier MTJs with a SyF to understand the factors affecting them. We have also investigated them in MgO-barrier MTJs with a single ferromagnetic recording layer (SF), as reference data.

2. Sample preparation

MTJ films were deposited onto SiO₂/Si substrates by rf magnetron sputtering. Two MTJ stacks (I and II), as shown in Fig. 1, were formed on Ta (5 nm) / Ru (10 nm) / Ta (5 nm) underlayers. Stack I(II) has a SF(SyF). Using electron-beam lithography and Ar-ion milling, stack I were first patterned into MTJs with four different junction sizes ($A = 0.15 \times 0.3$, 0.2×0.4 , 0.3×0.6 , and 0.6×1.2 μm^2), and stack II into those with $A = 0.08 \times 0.16$ μm^2 . Then all MTJs were annealed at 350°C for 1 h in a vacuum under a magnetic field of 4 kOe. From here on, MTJs fabricated from stack I and that from stack II are abbreviated to SF MTJs and SyF MTJs, respectively.

3. Results and discussion

After preparing a low resistance state by applying an external magnetic field, time dependent dielectric breakdown (TDDB) measurements were performed. Constant

voltage stresses are applied to the MTJs in the measurements because dielectric breakdown in MgO-barrier MTJs is dominated by electric field E rather than current density [4]. The direction of negative E applied to MTJs is shown in Fig. 2. Fig. 3 shows typical TDDB data; an abrupt decrease in resistance R is observed at $t = t_{BD}$. To calculate a cumulative fraction of broken MTJs (F) at t_{BD} , the measurements were repeated for about 50 MTJs. The distributions of t_{BD} in the SF MTJs with four different junction sizes are plotted on a Weibull scale (Fig. 4(a)). Fig. 4(b) is obtained by scaling the data points in Fig. 4(a) to an equivalent size of 0.6×1.2 μm^2 with $\ln(A)$ [5]. The data points ($\ln[-\ln(1-F)] \geq 0$) in Fig. 4(a), measured in the SF MTJs with different A , can be fitted with a straight line as shown in Fig. 4(b). Similar behavior is observed for positive E . This indicates that most of the breakdown sites are randomly distributed in the film plane. The slope β of the fitted line is $\beta = 0.32$; the value of β reflects the distribution of t_{BD} in the measured MTJs.

Fig. 6 shows Weibull plots for three different E stresses applied to the SyF MTJs. The data points can be fitted linearly with the slope $\beta = 1.4$. For positive E , the same value of β is obtained. The value of β in the SyF MTJs is about four times larger than that in the SF MTJs. This indicates that the spread of the distributions of t_{BD} in the SyF MTJs is narrower than that in the SF MTJs. We now discuss the factors leading to the difference in the value of β . There are four differences between the SyF and the SF MTJs: the junction size, the thickness of MgO, the layer structure of the recording layer, and the composition of CoFeB. Since Weibull plots are scaled well with A in the SF MTJs (Fig. 4(b)), we believe that the slope β holds for $A = 0.08 \times 0.16$ μm^2 . Thus, the present result is probably unrelated to A . The thickness of the MgO is also ruled out because β decreases as the oxide thickness is reduced [6]. Inhomogeneous stress acting on the MgO, which results in a reduction of the value of β , can be caused by a diffusion of B into the MgO from the CoFeB and a lattice mismatch between the crystallized CoFeB and the MgO. Since the diffusion of B is suppressed by a Ru layer employed in the SyF [7], and the lattice mismatch is reduced with a reduced Co concentration of the CoFeB [8], it seems that the Ru layer and/or the smaller Co concentration lead to the increased value of

β in the SyF MTJs.

Finally, we extrapolate the lifetime of the SyF MTJs from Fig. 5 assuming the E-model [9]. Negative E satisfying 63% or less failure in 10 years is 9.4 MV/cm (Fig. 6). The magnitude of E allows us to apply about 310 μ A to the MTJ, which is larger than the write current in the 2-Mb SPRAM [1].

4. Conclusions

Distributions of t_{BD} were investigated in MgO-barrier MTJs with a SyF and a SF. It is found that Weibull slope β in the SyF MTJs is larger than that in the SF MTJs. A comparison of them suggests that a Ru layer employed in the SyF and/or the smaller Co concentration of the CoFeB lead to the increased value of β in the SyF MTJs.

Acknowledgements

This work was partly supported by the “High-Performance Low-Power Consumption Spin Devices and Storage Systems” program under Research and Development for Next-Generation Information Technology of MEXT. The authors thank R. Sasaki, I. Morita, and T. Hirata for their technical support.

References

- [1] T. Kawahara *et al.*, JSSC **43** (2008) 109.
- [2] J. Hayakawa *et al.*, IEEE Trans. Mag. **44** (2008) 1962.
- [3] C. Yoshida *et al.*, Proc. of IRPS 2006 (2006) 697.
- [4] A. A. Khan *et al.*, J. Appl. Phys. **103** (2008) 123705.
- [5] J. Das *et al.*, J. Appl. Phys. **91** (2002) 7712.
- [6] R. Degraeve *et al.*, IEEE Trans. Electron Dev. **45** (1998) 904.
- [7] S. Pinitsoontorn *et al.*, Appl. Phys. Lett. **93** (2008) 071901.
- [8] K. Tsunekawa *et al.*, Jpn. J. Appl. Phys. **45** (2006) L1152.
- [9] W. Oepts *et al.*, J. Appl. Phys. **86** (1999) 3863.

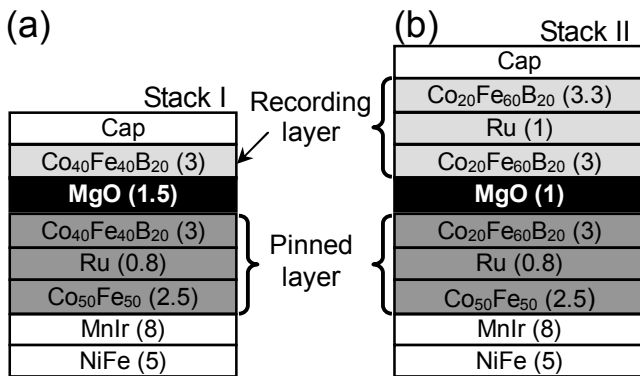


Fig. 1 Schematic diagrams of the MTJ stacks. The numbers in parentheses indicate the thickness in nm of the layers.

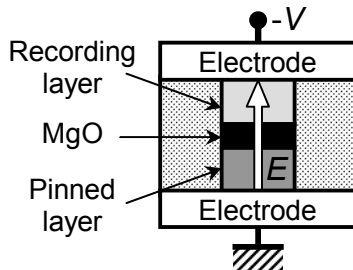


Fig. 2 Schematic diagram illustrating the direction of negative E .

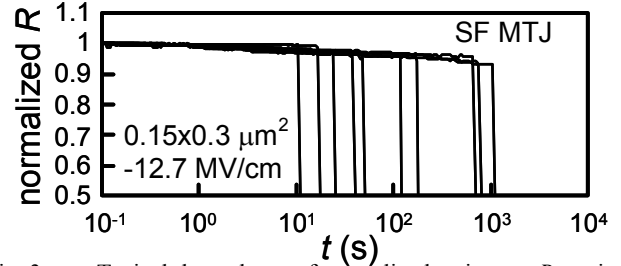


Fig. 3 Typical dependence of normalized resistance R on time t during the application of a stress electric field.

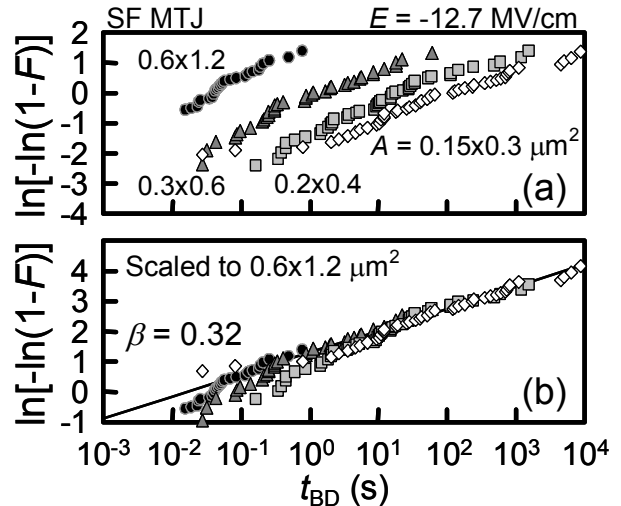


Fig. 4 (a) Weibull plots of t_{BD} in SF MTJs with four different junction sizes. (b) Weibull plots of t_{BD} , scaled to $0.6 \times 1.2 \mu\text{m}^2$.

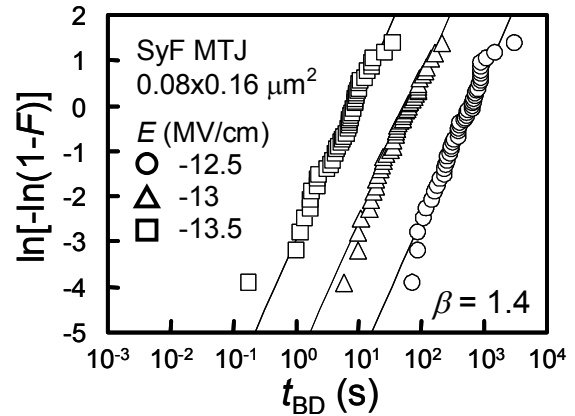


Fig. 5 Weibull plots of t_{BD} under negative E .

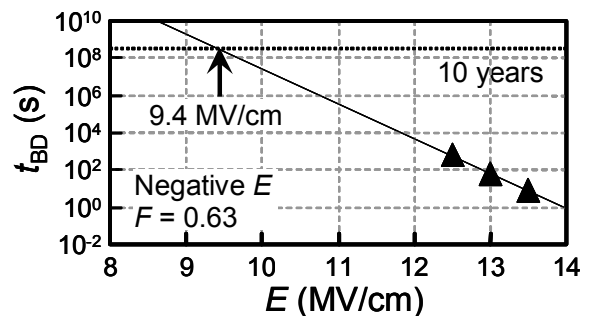


Fig. 6 Lifetime extrapolation under negative E in SyF MTJs.